

## **Laser Disdrometer (LDIS) Instrument Handbook**

D Wang

MJ Bartholomew

December 2023



## **DISCLAIMER**

This report was prepared as an account of work sponsored by the U.S. Government. Neither the United States nor any agency thereof, nor any of their employees, makes any warranty, express or implied, or assumes any legal liability or responsibility for the accuracy, completeness, or usefulness of any information, apparatus, product, or process disclosed, or represents that its use would not infringe privately owned rights. Reference herein to any specific commercial product, process, or service by trade name, trademark, manufacturer, or otherwise, does not necessarily constitute or imply its endorsement, recommendation, or favoring by the U.S. Government or any agency thereof. The views and opinions of authors expressed herein do not necessarily state or reflect those of the U.S. Government or any agency thereof.

# **Laser Disdrometer (LDIS) Instrument Handbook**

D Wang  
MJ Bartholomew  
Both at Brookhaven National Laboratory

Last updated: December 2023

How to cite this document:

Wang, D, and MJ Bartholomew. 2023. Laser Disdrometer (LDIS) Instrument Handbook. U.S. Department of Energy, Atmospheric Radiation Measurement user facility, Richland, Washington. DOE/SC-ARM-TR-137.

Work supported by the U.S. Department of Energy,  
Office of Science, Office of Biological and Environmental Research

## **Acronyms and Abbreviations**

AMF	ARM Mobile Facility
ARM	Atmospheric Radiation Measurement
CSV	comma-separated values
DOE	U.S. Department of Energy
DSD	drop size diameter
LDIS	laser disdrometer
LDQUANTS	Laser Disdrometer Quantities Value-Added Product
LWC	liquid water content
NetCDF	Network Common Data Form
SGP	Southern Great Plains
TRACER	Tracking Aerosol Convection Interactions Experiment
Z	reflectivity factor
ZDR	differential reflectivity

## Contents

Acronyms and Abbreviations .....	iii
1.0 Instrument Description .....	1
1.1 Technical Specifications .....	1
2.0 Data.....	3
2.1 Data Description.....	3
3.0 Historical Background.....	5
4.0 Maintenance Plan .....	6
5.0 Calibration Plan .....	7
6.0 User Notes and Known Issues .....	7
7.0 Citable References.....	8

## Figures

1 LDIS deployed at the TRACER (Tracking Aerosol Convection Interactions Experiment) main site (La Porte, Texas).....	1
2 Time series of rain rate, liquid water content (LWC), and radar reflectivity measured by LDIS at the TRACER main site (La Porte, Texas) on Aug 5, 2022. ....	4
3 Number of drops (in color) per diameter and fall velocity classes for LDIS 1-min raw data from June 2018 to December 2019 at the SGP C1 site.....	8

## Tables

1 Classification according to volume-equivalent diameter and fall speed. ....	2
2 Primary variables in b1-level ARM LDIS datastream. ....	4
3 Deployment information of LDIS in ARM.....	5

## 1.0 Instrument Description

The second-generation particle size velocity (Parsivel2, Figure 1) disdrometer, or laser disdrometer, referred to as 'LDIS' within the U.S. Department of Energy (DOE)'s Atmospheric Radiation Measurement (ARM) user facility, is a modern, laser-based disdrometer designed for comprehensive and reliable measurement of all types of precipitation. LDIS captures detailed information on the size and velocity of individual hydrometeors that fall to the ground, classifying them into a range of 32 categories.

These raw measurements are processed by a fast signal processor (provided by the vendor) to calculate various parameters, including precipitation type, amount, intensity, kinetic energy, visibility in the precipitation, and equivalent radar reflectivity. These measurements have served as the primary data set and a valuable reference for a variety of studies, ranging from observational analyses of precipitation processes and climate model evaluations to monitoring or validating radar/satellite retrievals (e.g., Wang et al. 2018, Giangrande et al. 2019, Jackson et al. 2020).



**Figure 1.** LDIS deployed at the TRACER (Tracking Aerosol Convection Interactions Experiment) main site (La Porte, Texas).

### 1.1 Technical Specifications

The LDIS used within ARM were manufactured by [OTT Hydromet GmbH](#), Kempten, Germany (Löffler-Mang and Joss 2000). The OTT Parsivel2, or LDIS, operates on the principle of extinction, quantifying precipitation particles through the shadowing effect they induce as they traverse a laser band. The transmitter unit emits a flat, horizontally oriented beam of light, which is subsequently converted into an electrical signal by the receiver unit. This signal undergoes changes whenever a hydrometeor passes through the beam within the measuring area. The extent of signal attenuation is indicative of the hydrometeor's size, and fall velocity is derived from the duration of the extinction signal.

The nominal measuring area of the LDIS is 54 cm<sup>2</sup>; however, a more precise characterization of the LDIS measurement area necessitates accounting for potential edge effects. In previous investigations (Wang et al. 2021), the effective sampling cross-section for the LDIS was defined as  $180 \times (30 - L/2)$ , where 'L' represents the size parameter.

The LDIS system offers measurements across 32 unevenly spaced bins for both drop size and fall velocity. It is essential to note that bin spacing is finer for smaller particles and those with slower fall velocities. The size and velocity ranges encompass values between 0.06 and 24.5 mm and 0.05 to 20.8 m/s, respectively. The class ranges are detailed in Table 1, with the caveat that classes 1 and 2 serve as boundaries and are not evaluated in OTT measurements, as they fall beyond the device's measurement range.

Precipitation type classification is determined based on the count of particles falling within the measurement range and is further categorized into eight distinct classes: drizzle, drizzle with rain, rain, rain and drizzle with snow, snow, snow grains, freezing rain, and hail.

The measured values by LDIS are characterized by a notable degree of precision, which remains consistent over an extended duration. This is facilitated by the ratiometric process, which inherently accounts for the effects of temperature characteristics and the aging of laser diodes, thus ensuring sustained accuracy.

**Table 1.** Classification according to volume-equivalent diameter and fall speed.

Class Number	Diameter Class Average (mm)	Diameter Class Spread (mm)	Velocity Class Average (m/s)	Velocity Class Spread (m/s)
1	0.062	0.125	0.050	0.100
2	0.187	0.125	0.150	0.100
3	0.312	0.125	0.250	0.100
4	0.437	0.125	0.350	0.100
5	0.562	0.125	0.450	0.100
6	0.687	0.125	0.550	0.100
7	0.812	0.125	0.650	0.100
8	0.937	0.125	0.750	0.100
9	1.062	0.125	0.850	0.100
10	1.187	0.125	0.950	0.100
11	1.375	0.250	1.100	0.200
12	1.625	0.250	1.300	0.200
13	1.875	0.250	1.500	0.200
14	2.125	0.250	1.700	0.200
15	2.375	0.250	1.900	0.200
16	2.750	0.500	2.200	0.400

Class Number	Diameter Class Average (mm)	Diameter Class Spread (mm)	Velocity Class Average (m/s)	Velocity Class Spread (m/s)
17	3.250	0.500	2.600	0.400
18	3.750	0.500	3.000	0.400
19	4.250	0.500	3.400	0.400
20	4.750	0.500	3.800	0.400
21	5.500	1.000	4.400	0.800
22	6.500	1.000	5.200	0.800
23	7.500	1.000	6.000	0.800
24	8.500	1.000	6.800	0.800
25	9.500	1.000	7.600	0.800
26	11.000	2.000	8.800	1.600
27	13.000	2.000	10.400	1.600
28	15.000	2.000	12.000	1.600
29	17.000	2.000	13.600	1.600
30	19.000	2.000	15.200	1.600
31	21.500	3.000	17.600	3.200
32	24.500	3.000	20.800	3.200

## 2.0 Data

### 2.1 Data Description

The raw data obtained from the ARM LDIS are primarily processed at the b1 level and are denoted by filenames following the format 'XXXldM1.b1.YYYYMMDD,' where 'XXX' represents the site name (e.g., 'houldM1.b1.20221001.000000'). These data are captured at one-minute intervals and are made available in netCDF and CSV formats through the [ARM Data Discovery tool](#).

The processed data include essential measurements, including precipitation intensity, weather code, equivalent radar reflectivity, the number of detected particles, particle size, liquid water content, intercept parameter, slope parameter, median volume diameter, number density of drops, and radar moments (An example is shown in Figure 2). A comprehensive list of variables is presented in Table 2. Additionally, the raw spectrum of the drop size distribution (DSD) is provided, with data organized by time, particle size bin, and fall velocity bin, allowing for the recalculation of radar moments and precipitation properties by researchers.

In instances where data is unavailable for a specific sample time, a 'missing\_value' of -999 is assigned to the corresponding field.



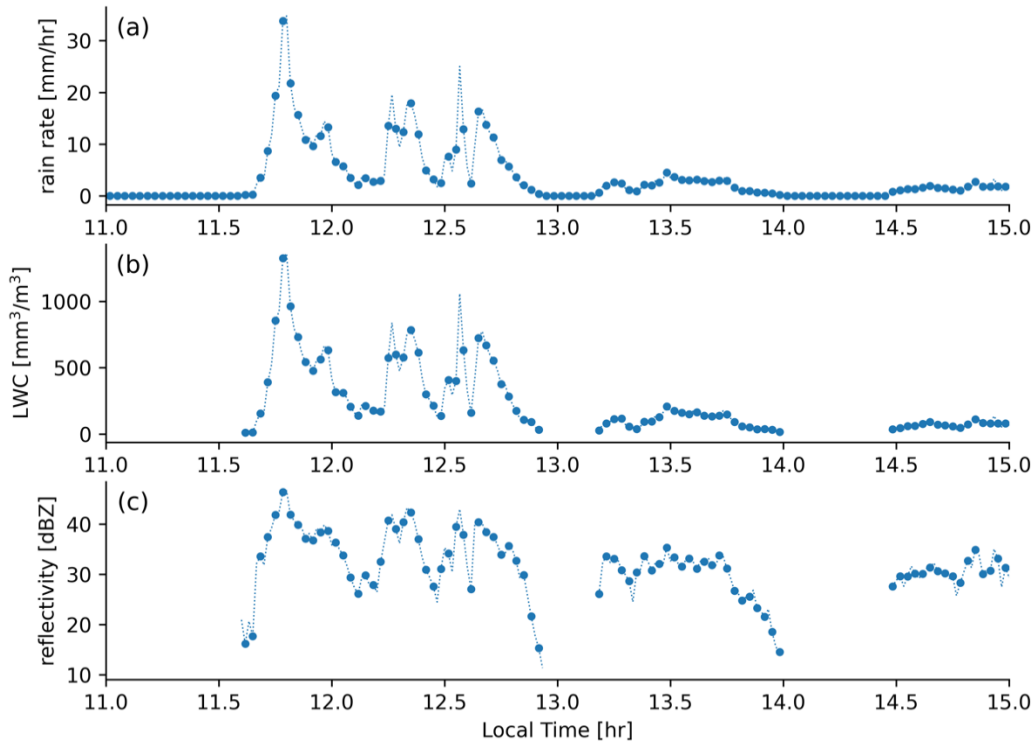


**Figure 2.** Time series of rain rate, liquid water content (LWC), and radar reflectivity measured by LDIS at the TRACER main site (La Porte, Texas) on Aug 5, 2022.

**Table 2.** Primary variables in b1-level ARM LDIS datastream.

Variable Name	Quantity	Unit
base_time	Base time in Epoch	seconds
time_offset	Time offset from base_time	seconds
time	Time offset from midnight	seconds
precip_rate	Precipitation intensity	mm/hr
diameter_min	Diameter of smallest drop observed	mm
diameter_max	Diameter of largest drop observed	mm
weather_code	SYNOP WaWa Table 4680	1
equivalent_radar_reflectivity_ott	Radar reflectivity from the manufacturer's software	dBZ
number_detected_particles	Number of particles detected	count
mor_visibility	Meteorological optical range visibility	m
snow_depth_intensity	Snow height	mm/hr
particle_size	Particle class size average	mm

Variable Name	Quantity	Unit
class_size_weight	Class size width	mm
raw_fall_velocity	Fall velocity classes observed	m/s
fall_velocity_calculated	Fall velocity calculated after Lhermite	m/s
raw_spectrum	Raw drop size distribution	count
liquid_water_content	Liquid water content	mm <sup>3</sup> /m <sup>3</sup>
equivalent_radar_reflectivity	Radar reflectivity calculated by ARM	dBZ
intercept_parameter	Intercept parameter, assuming an ideal Marshall-Palmer type distribution	l(m <sup>3</sup> mm)
slope_parameter	Slope parameter, assuming an ideal Marshall-Palmer type distribution	l/mm
median_volume_diameter	Median volume diameter, assuming an ideal Marshall-Palmer type distribution	mm
liquid_water_distribution_mean	Liquid water distribution mean, assuming an ideal Marshall-Palmer type distribution	mm
number_density_drops	Number density of drops of the diameter corresponding to a particular drop size class per unit volume	l(m <sup>3</sup> mm)
moment1	Moment 1 from the observed distribution	mm/m <sup>3</sup>
moment2	Moment 2 from the observed distribution	mm <sup>2</sup> /m <sup>3</sup>
moment3	Moment 3 from the observed distribution	mm <sup>3</sup> /m <sup>3</sup>
moment4	Moment 4 from the observed distribution	mm <sup>4</sup> /m <sup>3</sup>
moment5	Moment 5 from the observed distribution	mm <sup>5</sup> /m <sup>3</sup>
moment6	Moment 6 from the observed distribution	mm <sup>6</sup> /m <sup>3</sup>
lat	North latitude	degree N
N	East longitude	degree E
alt	Altitude above mean sea level	m

### 3.0 Historical Background

At present, ARM operates a total of eight LDIS across its fix sites in Oklahoma and the Azores as well as its three mobile facilities (AMFs). Deployment periods for these instruments are outlined in Table 3.

**Table 3.** Deployment information of LDIS in ARM.

Site Name	Field Campaign or Fixed Site	Location	Period
ENA	Eastern North Atlantic	Graciosa Island, Azores, Portugal	27 Feb.2014-present
MAO	Observations and Modeling of the Green Ocean Amazon (GOAMAZON)	Manacapuru, Amazonas, Brazil	24 Sep. 2014-1 Dec. 2015
SGP-CI	Southern Great Plains, Central Facility	Lamont, OK, USA	2 Nov. 2016-present
SGP-E13	Central Facility	Lamont, OK, USA	4 Nov. 2016-29 Sep. 2023

Site Name	Field Campaign or Fixed Site	Location	Period
SGP-I10	NW radar wind profiler site	Lamont, OK, USA	28 Nov. 2016-29 Sep. 2023
SGP-I9	SE radar wind profiler site	Billings, OK, USA	28 Nov. 2016-29 Sep. 2023
SGP-I8	NE radar wind profiler site	Tonkawa, OK, USA	5 Dec. 2016-29 Sep. 2023
COR	Cloud, Aerosol, and Complex Terrain Interactions (CACTI)	Cordoba, Argentina	23 Sep. 2028-1 May 2019
MOS-M1	Multidisciplinary Drifting Observatory for the study of arctic climate (MOSAIC)	Arctic region	14 Oct. 2019-20 Sep. 2020
MOS-S3	MOSAIC	Arctic region	17 Oct. 2019-16 Sep. 2020
HOU-M1	TRACER	La Porte, TX, USA	5 Aug. 2021-1 Oct. 2022
HOU-S1	TRACER	La Porte, TX, USA	18 Aug. 2021-2 Oct. 2022
HOU-S2	TRACER	Pearland, TX, USA	12 Apr. 2022-12 May 2022
HOU-S3	TRACER	Guy, TX, USA	5 May 2022-1 Oct. 2022
GUC-M1	Surface Atmosphere Integrated Field Laboratory (SAIL)	Gunnison, CO, USA	1 Sep. 2021-16 Jun. 2023
GUC-S2	SAIL	Gunnison, CO, USA	3 Sep. 2021-16 Jun. 2023
EPC-M1	Eastern Pacific Cloud Aerosol Precipitation Experiment (EPCAPE)	La Jolla, CA, USA	15 Jan. 2023-present
EPC-S2	EPCAPE	Mt. Soledad, CA, USA	15 Jan. 2023-present

## 4.0 Maintenance Plan

The maintenance plan for LDIS typically includes regular checks and cleaning of the instrument to ensure it continues to function accurately. Common maintenance tasks performed in ARM include:

1. Visual inspection: Regularly inspect the instrument for any physical damage, loose components, or signs of wear.
2. Cleaning the lenses: Clean the laser's protective lenses and surfaces to remove dirt, dust, or debris that may affect its measurements. Use a soft, lint-free cloth or a cleaning solution to clean the glass on both sensor heads from the outside. This process will be performed at least semiannually.
3. Keeping the light pathway open: At regular intervals, remove all impediments, such as leaves, branches, or spider webs that are in the way of the light pathway.
4. Cleaning the splash protection unit: Loosen the four hex screws of the respective splash protector using an M4 hex key and remove the splash protector. Then clean the protector using a brush and commercially available household cleanser on both sides under running water. Finally, reinstall the splash protector onto the respective sensor head using the hex screws.
5. Software and firmware updates: Keep the instrument's software and firmware up to date if updates are available from the manufacturer.

6. Documentation: Maintain records of maintenance activities, calibrations, and any issues encountered by maintenance report and/or Data Quality Problem Report.
7. Spare parts: Keep spare parts on hand to address any unexpected failures promptly.

## **5.0 Calibration Plan**

The instrument undergoes calibration by the vendor, and no calibration activities are conducted at the ARM sites. Nevertheless, prior to each deployment, we perform particle size measurement verification to ensure the instrument's proper functioning. This verification process can be executed either in the field or in a laboratory. It necessitates the use of reference spheres with known diameters, which are subsequently released at varying sizes through the center of the laser strip during a measurement interval of 60 seconds from a height of 0.25 meters. The obtained results should encompass all objects and their respective classifications based on both diameter and particle speed.

It is important to note that this verification method provides only an approximate assessment. In cases of uncertainty or doubt, we return the instrument to OTT for further inspection.

## **6.0 User Notes and Known Issues**

In the analysis of LDIS raw data, which, in this context, corresponds to b1 level data, it is not uncommon to encounter outliers. To ensure the highest data quality, these outliers must be effectively filtered out. For instance, some hydrometeors may fall on the periphery of the instrument's field of view, manifesting in the data as small drops that exhibit velocities exceeding their anticipated terminal fall rates. Alternatively, certain hydrometeors may enter the instrument's field of view after impacting the device, leading to the observation of larger drops with fall velocities that deviate from their expected terminal values. Moreover, spurious measurements can result from other objects such as insects, leaves, and spider webs.

The most prevalent outliers are typically identified and screened by removing data points with fall speeds that exceed or fall below 50% of the fall speeds derived from Tokay et al (2013) for raindrops (as shown in Figure 3). To enhance data quality and consistency, ARM undertakes post-processing of LDIS b1 level data by implementing these filters. The results of this post-processing are subsequently made available as c1 level data, [LDQUANTS](#).

In the Laser Disdrometer Quantities Value-Added Product (LDQUANTS) datastream, essential properties of the DSD are also computed. Specifically, various microphysical characteristics of raindrops, such as liquid water path, are derived by assuming either a gamma or exponential DSD distribution. To further facilitate the calibration of rain gauges and ground-based radar, this product computes radar-equivalent quantities, including dual-polarization radar parameters (e.g., Reflectivity Factor, Z, Differential Reflectivity, ZDR), employing the T-matrix scattering method.

It is worth noting that coincident hydrometeors are reported as a single entity, even in scenarios where multiple drops descend through the beam simultaneously. This practice may result in an underestimation of the drop counts (Yuter et al. 2006).

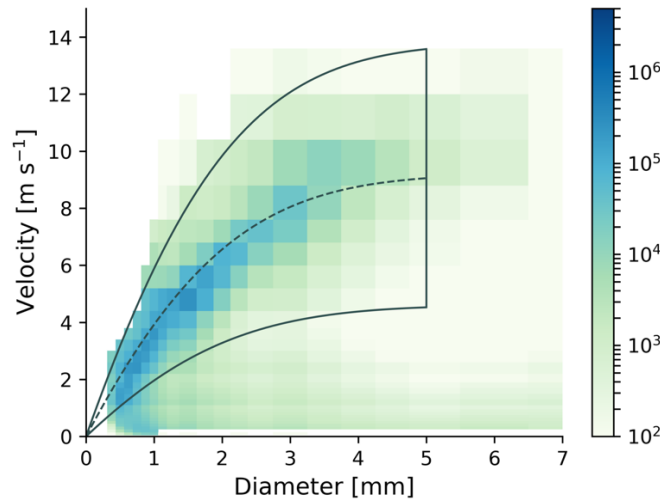


**Figure 3.** Number of drops (in color) per diameter and fall velocity classes for LDIS 1-min raw data from June 2018 to December 2019 at the SGP C1 site. The dashed curve represents the Tokay et al. (2013) terminal fall velocities, and the solid curves are  $\pm 50\%$  of the Tokay et al. (2013). The solid vertical line represents the 5-mm drop size threshold.

LDIS exhibits notable uncertainties when measuring frozen particles, such as snowflakes. The primary source of this uncertainty stems from the variation in axial ratios among frozen particles. Depending on the tilting angle and axial ratio of a particle as it traverses the LDIS field of view, the reported width can significantly differ from its actual width (Battaglia et al. 2010). For instance, in the case of frozen particles with a 2-mm diameter ( $D$ ), the ratio of the measured width to the true width can fluctuate between 0.6 and 1.6. For 5-mm particles, this ratio diminishes but still varies from 0.8 to 1.15. Likewise, the ratio of the observed fall velocity to the actual fall velocity ranges from 0.6 to 1.3 for 2-mm particles and from 0.4 to 2.0 for 5-mm particles.

Both particle size and fall speed serve as essential parameters for determining other DSD properties, such as precipitation intensity ( $R$ ) and radar reflectivity. The substantial uncertainties in measuring the particle size result in significant errors in the calculation of these DSD properties, particularly for higher radar moments like  $Z$ , as these calculations involve the sixth power of diameter.

## 7.0 Citable References

Battaglia, A, E Rustemeier, A Tokay, U Blahak, and C Simmer. 2010. “Parsivel snow observations: A critical assessment.” *Journal of Atmospheric and Oceanic Technology* 27(2): 333–344, <https://doi.org/10.1175/2009JTECHA1332.1>

Giangrande, SE, D Wang, MJ Bartholomew, MP Jensen, DB Mechem, JC Hardin, and R Wood. 2019. “Midlatitude Oceanic Cloud and Precipitation Properties as Sampled by the ARM Eastern North Atlantic Observatory.” *Journal of Geophysical Research – Atmospheres* 124(8): 4741–4760, <https://doi.org/10.1029/2018JD029667>

Jackson, R, S Collis, V Louf, A Protat, D Wang, S Giangrande, EJ Thompson, B Dolan, SW Powell, 2021. “The development of rainfall retrievals from radar at Darwin.” *Atmospheric Measurement Techniques* 14(1): 53–69, <https://doi.org/10.5194/amt-14-53-2021>

Löffler-Mang, M, and J Joss. 2000. “An optical disdrometer for measuring size and velocity of hydrometeors.” *Journal of Atmospheric and Oceanic Technology* 17(2): 130–139, [https://doi.org/10.1175/1520-0426\(2000\)0172.0.CO;2](https://doi.org/10.1175/1520-0426(2000)0172.0.CO;2)

Tokay, A, W Peterson, P Gatlin, and M Wingo. 2013. “Comparison of raindrop size distribution measurements by collocated disdrometers.” *Journal of Atmospheric and Oceanic Technology* 30(8): 1672–1690, <https://doi.org/10.1175/JTECH-D-12-00163.1>

Wang, D, SE Giangrande, MJ Bartholomew, JC Hardin, Z Feng, R Thalman, and LAT Machado. 2018. “The Green Ocean: precipitation insights from the GoAmazon2014/5 experiment.” *Atmospheric Chemistry and Physics* 18(12): 9121–9145, <https://doi.org/10.5194/acp-18-9121-2018>

Wang, D, Bartholomew, MJ, Giangrande, SE., and Hardin, JC. 2021. “Analysis of Three Types of Collocated Disdrometer Measurements at the ARM Southern Great Plains Observatory.” U.S. Department of Energy, Atmospheric Radiation Measurement user facility, Richland, Washington. DOE/SC-ARM-TR-275, <https://doi.org/10.2172/1828172>

Yuter, SE, DE Kingsmill, LB Nance, and M Löffler-Mang. 2006. “Observations of precipitation size and fall speed characteristics within coexisting rain and wet snow.” *Journal of Applied Meteorology and Climatology* 45(10): 1450–1464, <https://doi.org/10.1175/JAM2406.1>



[www.arm.gov](http://www.arm.gov)

U.S. DEPARTMENT OF  
**ENERGY**

---

Office of Science